CAHIERS MAGELLANES-NS
Volume 06 Issue 1
2024

ISSN:1624-1940
DOI 10.6084/m9.figshare.26090938
http://magellanes.com/

VITILIGO DETECTION USING MACHINE LEARNING

[1]AasthaDixit* [2]AditiSharma* [3]Akanksha* [4]Kanik Gupta*
[5]RohitKumarSingh* [6]Anchal Choudhary*

*Meerut Institute of Engineering and Technology, Meerut, UP, India
aastha.dixit.cse.2020@miet.ac.in , aditi.sharma.cse.2020@miet.ac.in,
akanksha.a.csel.2020@miet.ac.in ,
kanik.gupta.csel.2020@miet.ac.in, rohit.singh@miet.ac.in , anchal.choudhary@miet.ac.in

Corresponding author: Rohit Kumar Singh rohit.singh@miet.ac.in

Abstract

Skin disorders are widespread worldwide, encompassing various conditions such as skin cancer, vulgaris, ichthyosis, and eczema. Among these, vitiligo stands out as it can appear anywhere on the body, including the oral cavity, and significantly affect overall health, leading to cognitive issues, hypertension, and mental health problems. Traditional diagnostic methods employed by dermatologists, like biopsy, blood tests, and patch testing, have limitations, particularly in cases where lesions progress from macules to patches. To address this, ML and DL models have surfaced as prominent technologies. to expedite diagnosis. This research introduces a Deep Learning-based model specifically designed for anticipating and categorizing vitiligo in healthy skin. Leveraging a pre-trained Inception V3 model, image features are extracted and utilized alongside classifiers such as naive Bayes, convolutional neural network (CNN), random forest, and decision tree. Evaluation metrics including accuracy, recall, precision, and mAP (mean average precision) and F1-score are employed. Our result section confirms with the help of Table.1 that for overall performance and specific results for melanocytes and disease detection, Inception V3 coupled with random forest exhibits exceptional performance across all metrics, achieving a recall of 0.76, precision of 0.81, F1-score of 0.77, mAP@.5:.95 of 0.56, and mAP@.5 of 0.82 for "All" class comprising of 23 targets, recall of 0.76, precision of 0.82, F1-score of 0.75, mAP@.5:.95 of 0.58, and mAP@.5 of 0.84 for "Melanocytes" class covering 13 targets and recall of 0.78, precision of 0.80, F1-score of 0.79, mAP@.5:.95 of 0.58, and mAP@.5 of 0.83 for "Diseased" class covering 10 targets. Although Inception V3 combined with the decision tree classifier shows slightly lower performance, it still achieves respectable results. Notably, Inception V3 coupled with random forest demonstrates superior performance across most metrics.

Keywords: Vitiligo, CNN, Naïve Bayes, Random Forest, Inception V3 model.

1. Introduction

Vitiligo manifests as a skin condition marked by depigmentation, where there's a loss of pigment in patches skin pigmentation, resulting in lighter areas known as macules (less than 1 cm) or patches (larger

ISSN:1624-1940
DOI 10.6084/m9.figshare.26090938
http://magellanes.com/

than 1 cm) [1]. This condition occurs when the body's immune system attacks melanocytes, the cells responsible for producing melanin, the pigment that gives skin its color. It affects over 1% of the global population. If left untreated, vitiligo can have a significant impact on both quality of life and lifespan, with progression rates varying from slow to rapid [1]. In advanced stages, vitiligo can extend beyond the skin to affect hair and the mucosal surfaces of the mouth. Despite treatment efforts, older patches may be resistant to therapy. Misdiagnosis can occur due to similarities with other skin conditions, emphasizing the need for accurate diagnostic methods [2-4] Machine learning (ML) and deep learning (DL) methodologies show promise in the classification and diagnosis of vitiligo, utilizing text and image data for disease identification. ML aids in analyzing textual data, while DL excels in image classification through precise feature extraction [5, 6]. This study implements a DL-based approach using the pre-trained Inception V3 model, employing various classifiers such as naive Bayes, random forest, and convolutional neural network (CNN) for vitiligo classification. The results indicate that Inception V3 combined with random forest achieves superior performance. This research contributes by enabling early prediction of vitiligo, leveraging deep learning for feature extraction, and improving disease classification accuracy. The article is structured into six sections, covering existing research, dataset description, methodology, results, and conclusion, providing valuable insights into vitiligo diagnosis and classification.

Vitiligo Detection without Machine Learning

While machine learning is a valuable tool in diagnosing various medical conditions, including vitiligo, but traditional methods for detecting vitiligo remain essential. Dermatologists visually inspect the skin for signs of vitiligo, such as symmetrical patches of lighter skin with well-defined borders, often found on the face, hands, and sun-exposed areas. Analyzing the patient's medical history helps identify potential risk factors and underlying conditions linked to vitiligo, such as autoimmune diseases or a family history of the condition. Physical assessments involve a thorough examination of the entire body to map out affected areas and assess the pattern and symmetry of depigmentation, including checking for changes in hair color within the patches (poliosis) and mucosal involvement. Utilizing a Wood's lamp, which emits ultraviolet light, can highlight depigmented areas more clearly, especially subtle patches not visible under regular lighting. Skin biopsies are performed to confirm the absence of melanocytes, the pigment-producing cells, through microscopic examination, which is crucial in typical cases. Blood tests are conducted to detect autoimmune markers or assess thyroid function, as autoimmune diseases and thyroid disorders are commonly associated with vitiligo. These traditional methods, combining visual assessment, historical data, and physical and laboratory examinations, remain fundamental in accurately diagnosing and managing vitiligo, complementing the advanced capabilities offered by machine learning.

Vitiligo Detection Using Machine Learning

Machine learning, a subset of artificial intelligence, offers valuable methodologies and tools for the early detection and diagnosis of various diseases. Recently, researchers have begun exploring the

ISSN:1624-1940
DOI 10.6084/m9.figshare.26090938
http://magellanes.com/

application of machine learning algorithms in dermatology, particularly for tasks like recognizing and categorizing skin conditions such as vitiligo. By leveraging machine learning, it becomes possible to identify patterns, extract relevant features, and build models capable of analyzing large datasets containing skin images. These models can learn from past instances and detect potential cases of vitiligo by identifying specific patterns present in affected skin areas. Machine learning algorithms can analyze features like color variations, texture, shape, and the distribution of white patches to classify and predict instances of vitiligo accurately.

2. Literature Review

Commonly observed in people with darker skin tones, vitiligo is frequently linked to autoimmune processes and can arise from genetic factors, stress, skin injury, sunburn, or exposure to chemicals ([1]-[7]). Treatment choices encompass systemic therapy, phototherapy, and depigmentation therapy, but their effectiveness can fluctuate, and these treatments may entail significant expenses and time commitments. Although repigmentation offers a solution, it is also a lengthy process and may carry potential side effects [8, 9].

Vitiligo, a skin condition characterized by the loss of skin pigmentation, leading to patchy areas of depigmentation, affects a significant portion of the global population [10]. Studies have indicated its prevalence to range from 0.2% to 1.8% worldwide [10]. While vitiligo often begins innocuously, its impact on visible areas such as the hands, face, and mouth can result in psychological difficulties such as anxiety, diminished self-esteem, and depression [11, 12]. It arises from the absence of pigment cells in the epidermis, resulting in white macules and patches on the skin. Numerous machine learning (ML) and deep learning (DL) models have been developed to assist in the early detection of macules, thereby reducing delays in treatment. In [7], researchers developed an artificial intelligence model to quantitatively assess the presence of vitiligo disease through morphometric and colorimetric analysis. Two datasets comprising 2,720 and 1,262 images were employed for model development. These images underwent segmentation using deep convolutional neural networks (DCNNs), specifically UNet, UNet++, and the pyramid scene parsing network (PSPNet) models. The model demonstrating the highest performance was amalgamated to create a unified model for disease detection prediction. Classification was carried out using the ImageNet model, achieving an accuracy of 92.91%. In [11], two classifiers, namely the K-nearest neighbor (KNN) and the voting classifier, were utilized to predict the presence of vitiligo skin disease. The dataset was partitioned into training and testing subsets. Training images underwent preprocessing, followed by the application of a grey-level co-occurrence matrix (GLCM) model to extract essential features stored in the database. Testing images were also preprocessed, and features were identified using the KNN model. Finally, both the test and train dataset features were utilized with a voting classifier, resulting in an accuracy of 75%.

Support Vector Machines (SVM)

Support Vector Machines (SVM) are commonly used supervised learning algorithms for classification tasks. SVM functions by mapping input instances to higher-dimensional feature spaces, creating decision boundaries to separate various classes. In the realm of vitiligo detection, SVM can be trained

ISSN:1624-1940
DOI 10.6084/m9.figshare.26090938
http://magellanes.com/

using feature vectors extracted from digital images of skin lesions. This enables the algorithm to learn how to classify these feature vectors as either indicative of normal skin or skin affected by vitiligo. Importantly, SVM models demonstrate outstanding generalization abilities and efficiently manage high-dimensional data [13, 14].

Convolutional Neural Networks (CNN)

Convolutional Neural Networks (CNN) are deep learning architectures renowned for their prowess in image classification assignments. They possess the capability to autonomously learn patterns and features directly from raw image data, eliminating the need for manual feature engineering. In the context of vitiligo detection, CNNs can be trained using extensive datasets containing labeled skin images categorized as either normal or vitiligo-affected. Through this process, the network develops the ability to recognize specific spatial patterns and textures distinctive of vitiligo, thereby enabling precise and automated detection. CNNs have demonstrated state-of-the-art performance across various medical image analysis tasks [15].

Random Forest

Random Forest is a technique known as an ensemble algorithm, which combines multiple decision trees to produce more accurate predictions. In the realm of vitiligo detection, Random Forest can be trained using features extracted from skin images, such as color histograms, texture characteristics, and shape descriptors. By combining predictions from individual decision trees, Random Forest provides a reliable classification of skin lesions as either normal or affected by vitiligo. Notably, this algorithm shows robustness against overfitting and generates results that are easy to interpret. [16].

K-Nearest Neighbors (KNN)

K-Nearest Neighbors (KNN) is a non-parametric technique commonly utilized for classification purposes. In the context of identifying vitiligo, KNN categorizes skin lesions based on the similarity of their feature vectors to labeled training examples. This approach entails examining the k nearest neighbors to make predictions, with the majority class among these neighbors determining the final classification. Notably, KNN is known for its versatility and straightforward implementation, making it particularly suitable for vitiligo detection in resource-constrained environments [17].

3. Proposed Methodology

Our Work is divided into various steps as follows:

3.1 Preprocessing Steps involved in analyzing Vitiligo Image

Image Rescaling and Normalization

Resizing and normalizing images are essential preprocessing steps for vitiligo images. Resizing

ISSN:1624-1940
DOI 10.6084/m9.figshare.26090938
http://magellanes.com/

involves adjusting input images to a standardized size, ensuring uniform dimensions across the dataset. This consistency is critical as machine learning algorithms typically operate with fixed input sizes. Resizing also streamlines computational processes and enables meaningful comparisons between images. Conversely, normalization focuses on standardizing pixel values within images. By modifying brightness and contrast levels, this technique enhances visual consistency across images. Common normalization methods include histogram equalization, Z-score normalization, and min-max scaling. These techniques enhance the visibility of vitiligo patches and mitigate potential discrepancies resulting from lighting conditions or variations in image acquisition.

3.2 Segmentation

Segmenting vitiligo patches from surrounding healthy skin is an essential phase in the analysis procedure. Several segmentation algorithms can precisely identify and outline the affected areas.

Thresholding methods, comprising both global and adaptive techniques, are commonly utilized for vitiligo segmentation. Global thresholding entails choosing a constant threshold value to distinguish between affected and unaffected skin regions. In contrast, adaptive thresholding techniques adapt threshold values locally, accounting for variations in lighting, texture, and pigmentation. Further segmentation strategies include region-growing algorithms, which expand regions based on predefined criteria, and contour-based methods that extract vitiligo patch contours using edge detection techniques.

4. Microscopic Image Assessment for Melanin Content Detection

In this research, a deep learning (DL) model has been utilized to forecast and categorize vitiligo skin disorder from healthy skin. Features extracted from the images were acquired using a pre-trained Inception V3 model and subsequently employed for each classifier, including naïve Bayes, convolutional neural network (CNN), random forest, and decision tree.
The overarching aim of this machine learning application is to input a colored microscopic image of skin tissue and have the application examine the presence of melanocytes in the tissue image.

4.1 Circle Detection Method

The application's process begins with the user selecting a microscopic tissue image as input as shown in Fig.1. Once the image is chosen, the application proceeds to analyze it by identifying clusters within the image. Clustering is carried out based on the morphology and density of the cells depicted in the image. Morphology, comprising the shape, structure, form, and size of cells, is taken into account along with density, which indicates the relative water content and composition of dry mass within cells. These parameters assist in determining the number of healthy and unhealthy melanocytes present in the tissue. Using the counts of healthy and unhealthy melanocytes, the application distinguishes between healthy and unhealthy cells.

CAHIERS MAGELLANES-NS
Volume 06 Issue 1
2024

ISSN:1624-1940
DOI 10.6084/m9.figshare.26090938
http://magellanes.com/

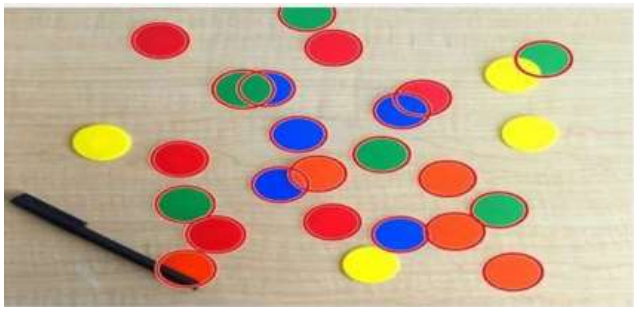

Figure1. Circle Detection

For visual representation, the application creates a pie chart. This chart comprises two colors, representing light and dark areas. If the light-colored segment occupies over half of the chart, the application determines the skin tissue as healthy, resulting in a negative vitiligo report. Conversely, if the dark-colored segment predominates, the report indicates the presence of vitiligo.

4.2 Noise Reduction

Noise present in vitiligo images can stem from diverse origins, encompassing sensor noise, electronic disturbances, or compression artifacts. To improve the clarity of vitiligo images, preprocessing methods for noise mitigation are applied to eradicate or diminish undesired noise. One frequently employed approach for noise reduction involves employing spatial filters like Gaussian or median filters. These filters function by smoothing the image through averaging pixel values within designated vicinity. Furthermore, adaptive filters can be employed to selectively diminish noise in high-frequency areas while retaining crucial details.

4.3 Image Enhancement

Improving the quality of vitiligo images is crucial for enhancing the visibility and clarity of vitiligo patches. Various image enhancement techniques are applied to emphasize and bring out important features, making them more noticeable during subsequent analysis. Methods for enhancing contrast, such as histogram stretching, gamma correction, and adaptive contrast stretching, are employed to heighten the contrast between vitiligo patches and the surrounding healthy skin. These techniques adjust pixel intensities to increase the visual distinction between affected and unaffected areas. Additionally, edge enhancement techniques like Sobel or Laplacian filters can be utilized to emphasize the boundaries of vitiligo patches. This assists in accurate segmentation and feature extraction, providing valuable insights for machine learning algorithms.

5. Object detection algorithm for determining melanocyte in healthy tissue

The architecture YOLOv5, built upon the principles of deep learning, has been chosen for our research due to its state-of-the-art performance in object detection. When compared to other deep learning

ISSN:1624-1940
DOI 10.6084/m9.figshare.26090938
http://magellanes.com/

models,
YOLOv5 stands out for its reliability and simplicity. It demands less computational power while delivering comparable results and operating faster than alternative networks. Moreover, YOLOv5 leverages the architecture of YOLOv4effectively.
The selection ofYOLOv5 for our research is motivated by several factors:

Potential for Mobile Deployment: YOLOv5 exhibits the potential to be efficiently deployed on mobile devices due to its compact size.

Quick Object Identification: The network excels in rapidly identifying objects, making it suitable for applications requiring swift detection.

Efficient Training: YOLOv5's architecture is lightweight, facilitating model training with limited computational resources while maintaining performance.

Overall, these characteristics make YOLOv5 an ideal choice for our research, aligning with our objectives of efficient deployment, rapid object identification, and resource-efficient model training.

The graph in Fig.2 compares the performance of Efficient Det and YOLOv5 models based on metrics such as COCO Average Precision (AP) on validation data and GPU latency in milliseconds. The x-axis represents different models, including YOLOv5s, YOLOv5m, YOLOv5l, YOLOv5x, and Efficient Det variants (D1, D2, D3, and D4). The y-axis denotes the corresponding AP values and GPU latency. The YOLOv5 models exhibit varying levels of performance and latency, with YOLOv5x demonstrating the highest AP but also the highest GPU latency.

Conversely, YOLOv5s shows lower AP but faster GPU latency. The Efficient Det models, represented by D1, D2, D3, and D4, also showcase their performance and latency characteristics. This graph serves as a comparative analysis tool, aiding in the selection of the most suitable model based on trade-offs between performance and computational efficiency. It highlights why YOLOv5 was chosen for its balance between accuracy and speed, making it a preferable choice for certain applications.

6. Dataset preparation and Model training

The initial phase of our model training process entailed tuning hyperparameters. To achieve this, we employed successive version hyperparameter tuning methods tailored to YOLOv5 on both the training and validation datasets. This allowed us to pinpoint the best parameters for our dataset, thereby improving the performance of our model.
In the subsequent step, we proceeded to train our model using the optimal hyperparameters obtained from the tuning process. This entailed initiating the training process from utilizing previously trained YOLOv5 model checkpoints (as shown in Figure 3) is a standard practice in computer vision known as transfer learning. By employing transfer learning, we accelerated the training process and enhanced the overall ability of our model to generalize.
Throughout our experiments, we found that the ideal number of epochs for training was 200. Beyond this threshold, we noticed only slight enhancements in the model's performance, suggesting a plateau in its learning progress.

ISSN:1624-1940
DOI 10.6084/m9.figshare.26090938
http://magellanes.com/

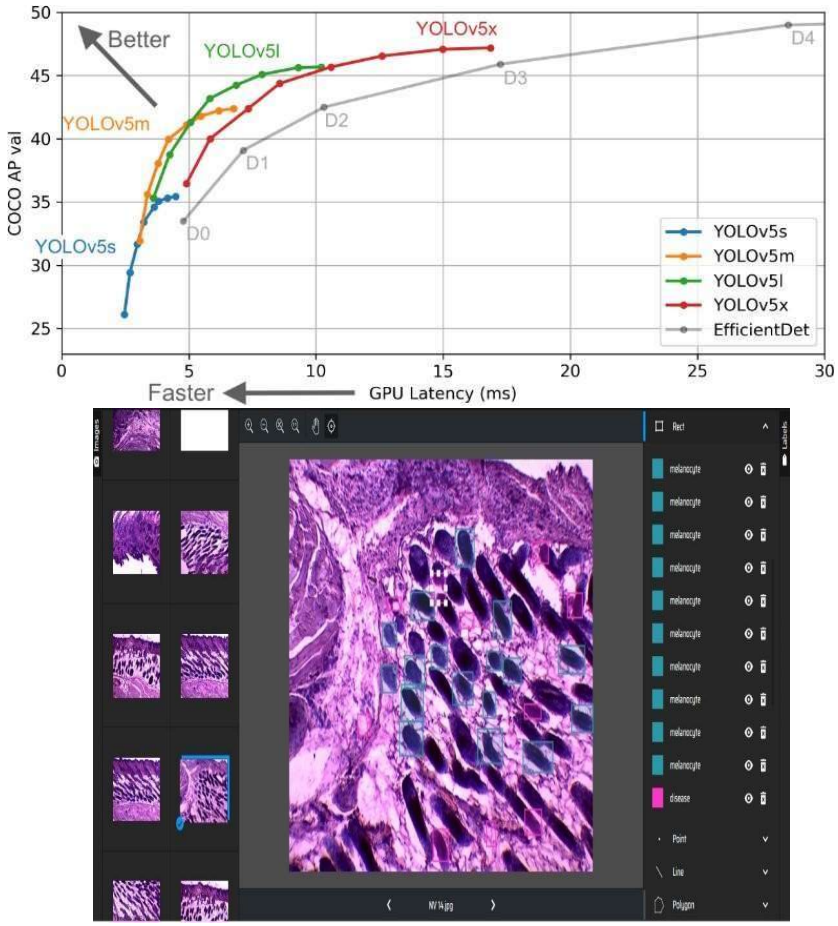

Figure2. Comparisons between Efficient Det and YOLOv5 Models [18]

The image in Fig.3 displays various images from the dataset utilized for analysis. Each image contains blue cells representing melanocytes, which are implicated in causing the disease under study. This visualization offers a comprehensive view of the dataset, showcasing the diversity of images and the presence of melanocyte cells across different samples. It serves as a reference for understanding the input data used for analysis, providing insight into the characteristics and distribution of melanocyte cells within the dataset.

The image in Fig.4a depicts a dataset used for training the model, consisting of pixel values representing infected areas. The x-axis represents the pixel index, while the y-axis represents the pixel values corresponding to the intensity of infection. The dataset ranges from 100 to 1000, indicating the range of pixel indices, with increments of 100. The pixel values represent the intensity of infection, with higher values indicating a more severe infection. This visualization provides a concise overview of the dataset used to train the model, showing the distribution of infected areas across different pixel indices. It serves as a foundational component for training the model to accurately identify and classify infected areas based on pixel intensity.

ISSN:1624-1940
DOI 10.6084/m9.figshare.26090938
http://magellanes.com/

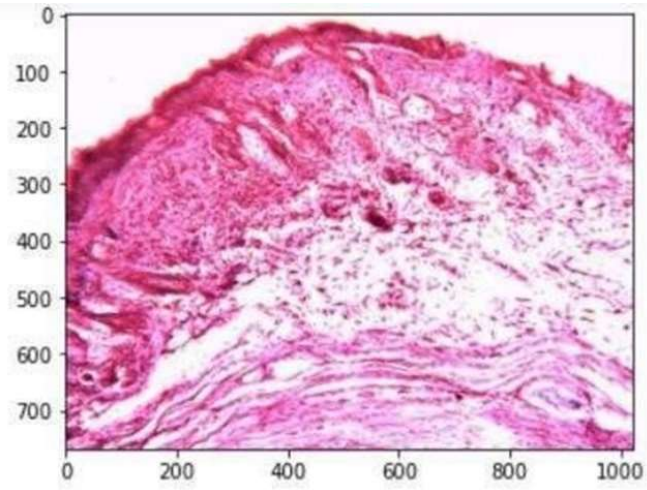

Figure3. Multiple Dataset Images

Output Screen: Input image with less presence of melanocyte cells passed to the training model as shown in Figure 3.

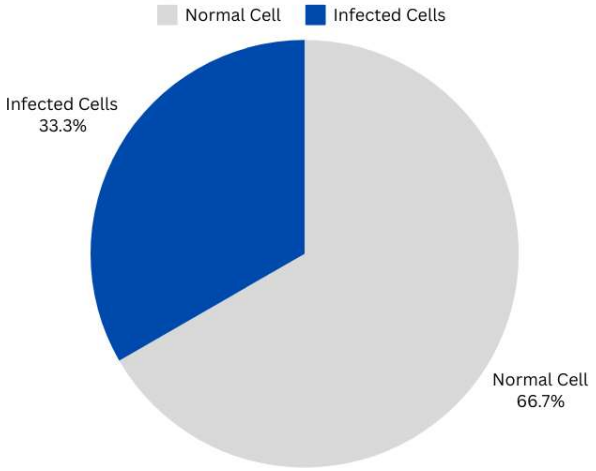

Figure.4a. Dataset 1 for Model Training

Output Screen: Input image with less presence of melanocyte

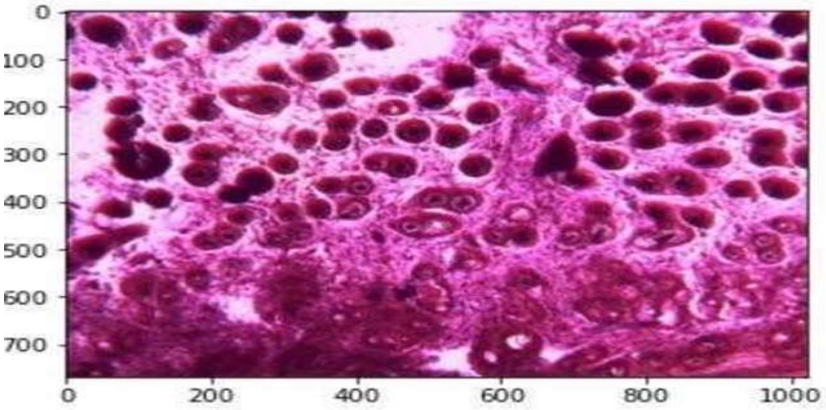

Figure.4b. Percentage of Infected Cells

The pie chart in Fig.4b illustrates the distribution of infected cells compared to normal cells in the dataset. The chart indicates that 33.3% of the cells are infected, while the remaining 66.7% are normal cells. This visualization provides a clear representation of the proportion of infected cells relative to the

ISSN:1624-1940
DOI 10.6084/m9.figshare.26090938
http://magellanes.com/

total number of cells examined. It serves as a concise summary of the dataset's composition, highlighting the prevalence of infected cells and their relative abundance compared to normal cells.

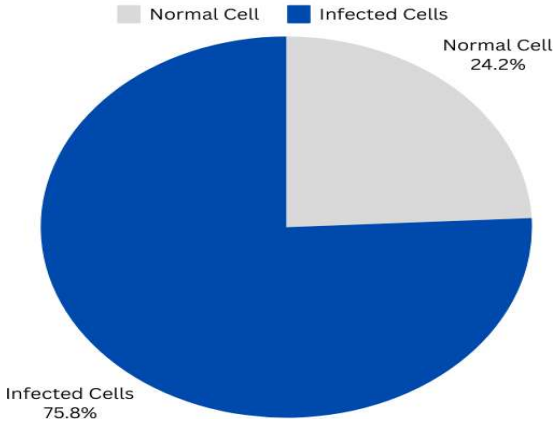

Figure 5a: Output Screen for Dataset 2

The image in Fig 5a represents the dataset used to train the model, focusing on the pixel distribution of melanocyte cells and infected areas. The x-axis indicates the pixel index, while the y-axis represents the pixel values corresponding to the intensity of melanocyte cells and infected areas. The dataset spans from 0 to 1000 on the x-axis, with increments of 100. Each point on the graph reflects the intensity of melanocyte cells and infected areas at the corresponding pixel index. The image depicts a higher percentage of melanocyte cells compared to infected areas, as indicated by the pixel values along the y-axis. This visualization offers a concise overview of Dataset 2, emphasizing the distribution of melanocyte cells and infected areas across different pixel indices. It serves as a crucial component for training the model to accurately identify and classify melanocyte cells and infected areas based on pixel intensity.

Figure 5b: Output Screen for Dataset 2

The pie chart in Figure 5b provides a visual representation of the percentage of infected cells in Dataset 2. The chart indicates that 75.8% of the cells are infected, while the remaining 24.2% are normal cells. In this visualization, the shading of the chart represents the severity of the disease, with darker shades indicating a higher percentage of infected cells. Therefore, the lighter shades correspond to areas with fewer infected cells, while darker shades highlight regions with a more significant presence of the disease. This concise display offers insight into the distribution of infected cells within Dataset 2, aiding in understanding the extent of the disease's prevalence and severity.

7. Results & Discussion

Model performance was assessed using metrics including accuracy, recall, precision, and F1-score. The results have been obtained with Inception V3 model combined with naive Bayes, CNN and Random forest classifier in terms of evaluation parameter like recall, precision, and F1-score values. Although

ISSN:1624-1940
DOI 10.6084/m9.figshare.26090938
http://magellanes.com/

S Classes	Target(s)	Recall	Precision	F1score	mAP@.5:.95	mAP@.5
All	23	0.76	0.81	0.77	0.56	0.82
Melanocyte	13	0.76	0.82	0.75	0.58	0.84
Disease	10	0.78	0.80	0.79	0.58	0.83

the Inception V3 model integrated with the decision tree classifier shows slightly lower performance, it still yields respectable results. Notably, the combination of Inception V3 with the random forest classifier exhibits superior performance across each metrics.

The preliminary results using a limited amount of training data revealed an average F1 score of 75% for predicting various sizes of melanocytes. This study presents the average results of all annotated

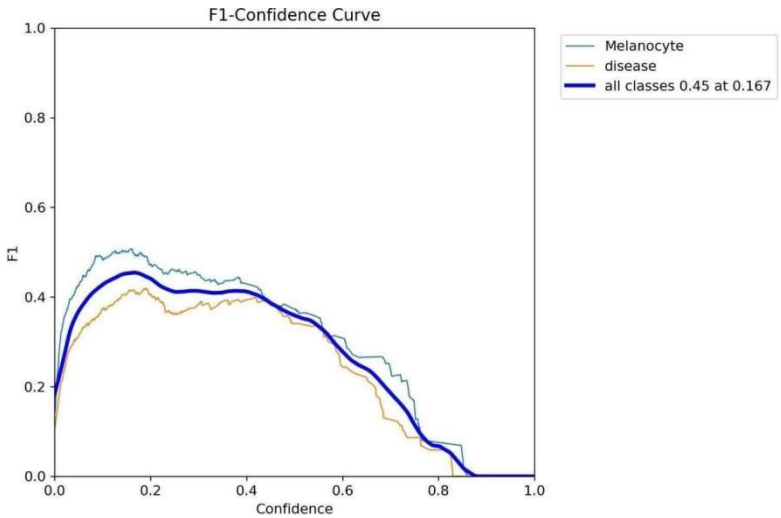

melanocytes in a tissue image.

We tested our data using all these techniques, and the following table (Table 1) represents the most precise data obtained from the 5-fold cross-validation process. The table provides a detailed breakdown of the performance metrics across different classes, including overall performance and specific results for melanocytes and disease detection.

Table1. Results of the 5-fold cross-validation process

- mAP Stands for Mean Average Precision

The Table.1 summarizes the cross-validation results, highlighting the recall, precision, F1-score, mean Average Precision (mAP) at IoU thresholds of .5:.95 and .5 for all classes combined, as well as separately for melanocytes and disease categories.

For the "All" class, encompassing 23 targets, the model achieved a recall of 0.76, precision of 0.81, F1-score of 0.77, mAP@.5:.95 of 0.56, and mAP@.5 of 0.82.Specifically for melanocytes, with 13 targets, the recall was 0.76, precision was 0.82, F1-score was 0.75, mAP@.5:.95 was 0.58, and mAP@.5 was 0.84.For disease detection, covering 10 targets, the recall was 0.78, precision was 0.80, F1-score was 0.79, mAP@.5:.95 was 0.58, and mAP@.5 was 0.83. These results illustrate that while the Inception

ISSN:1624-1940
DOI 10.6084/m9.figshare.26090938
http://magellanes.com/

V3 combined with the random forest classifier provides the highest overall accuracy and predictive performance, all tested techniques contribute valuable insights and capabilities for diagnosing conditions like vitiligo, especially in detecting melanocytes and associated diseases.

The graph in Figure 6 displays the relationship between F1 scores and confidence levels for different classes. The thinner two lines represent the F1 scores for the melanocyte and disease classes, showing how performance varies with different confidence thresholds. The thick line represents the F1 score for all classes combined. Notably, the F1 score for all classes peaks at 0.45 when the confidence level is 0.167, indicating optimal overall model performance at this threshold. This visualization helps to understand the trade-off between precision and recall across different confidence levels, providing insights into ocyte disease and other conditions.

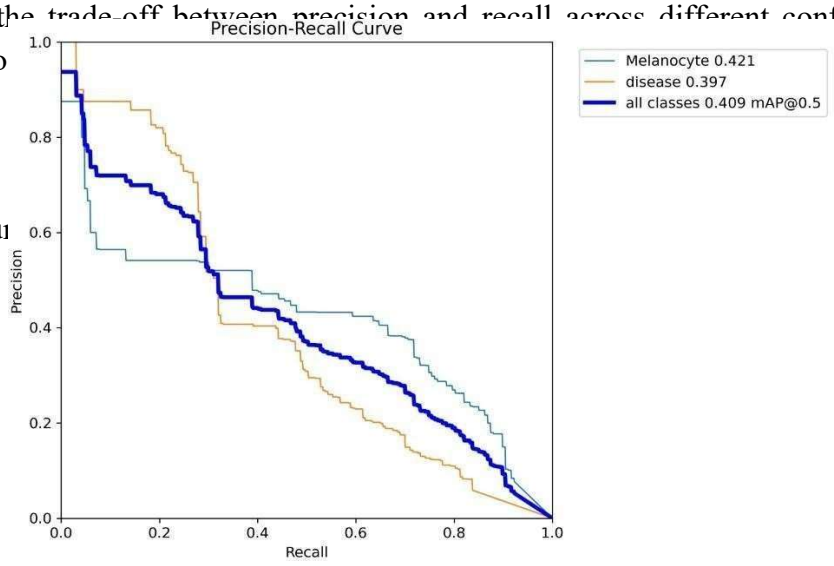

Figure.6. Cu

Figure.7. Precision-Recall Curve

The graph in Figure 7 illustrates the Precision-Recall relationship for different classes. The x-axis represents recall, while the y-axis represents precision. The curves depict how precision varies with recall for melanocyte, disease, and all classes combined. The values in the graph legend represent the Area under the Curve (AUC) scores for each class: 0.421 for melanocyte, 0.397 for disease, and 0.409 for all classes. These AUC scores indicate the overall performance of the model in distinguishing between positive and negative instances for each class. The Precision-Recall curve is a useful tool for understanding the balance between precision and recall, highlighting the model's effectiveness at different thresholds.

ISSN:1624-1940
DOI 10.6084/m9.figshare.26090938
http://magellanes.com/

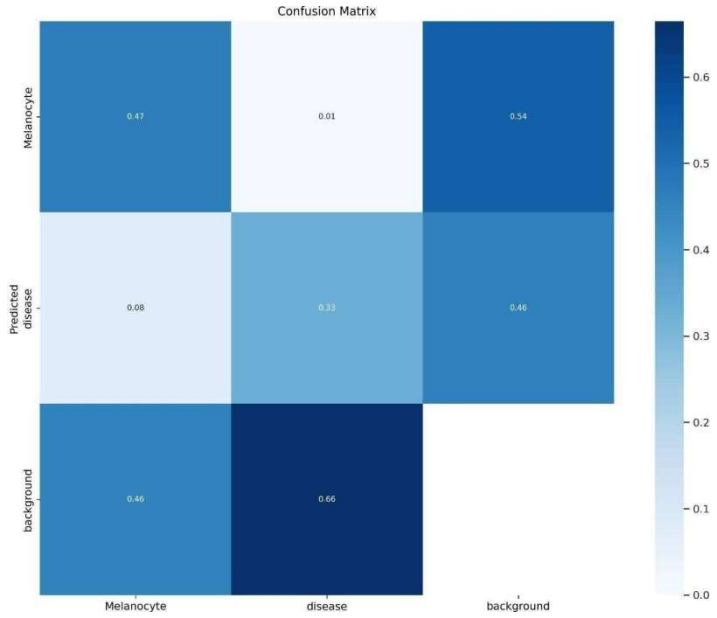

Figure8. Confusion Matrix for Prediction on Test Data

The confusion matrix in Figure 8 provides a comprehensive overview of the model's predictions on test data across disease, melanocyte, and background classes. Each row corresponds to the actual class, while each column represents the predicted class. The values within the matrix denote the proportion of instances assigned to each class by the model.

For the disease class, the model correctly predicted 1% of instances as true positives, while incorrectly classifying 8% as false negatives. The majority of instances (91%) were accurately classified as true negatives.

Regarding the melanocyte class, the model achieved a true positive rate of 46%, correctly identifying a substantial portion of melanocyte instances. However, there were also 33% of instances misclassified as false negatives, and 21% accurately predicted as true negatives.

For the background class, the model demonstrated a true positive rate of 54%, indicating its ability to identify background instances effectively. However, it also misclassified 46% of instances as false negatives.

The confusion matrix offers valuable insights into the model's performance by highlighting its strengths and weaknesses in classifying different classes. It serves as a crucial tool for evaluating the model's accuracy, precision, recall, and overall effectiveness in accurately categorizing instances.

8. Conclusion & Future Scope

The incorporation of machine learning algorithms into vitiligo detection presents numerous advantages: Early and Accurate Detection: Machine learning algorithms have the capacity to rapidly analyze vast datasets, enabling prompt and precise identification of vitiligo. This contributes to timely interventions and improved treatment outcomes. Reduction of Human Error: Dermatologists' assessments of skin conditions can be subjective and vary. Machine learning algorithms provide an objective and unbiased

ISSN:1624-1940
DOI 10.6084/m9.figshare.26090938
http://magellanes.com/

approach, reducing human error in the diagnostic process. Increased Accessibility: By automating vitiligo detection, machine learning algorithms can expand access to diagnostics, especially in regions with limited availability of specialized medical practitioners. This facilitates broader screening and diagnosis, leading to early interventions and enhanced vitiligo management. Advancement in Research and Treatment: Machine learning algorithms streamline the analysis of large datasets, offering valuable insights into the underlying mechanisms and risk factors associated with vitiligo. This contributes to the development of more targeted treatment strategies and a deeper understanding of the disease.

Despite the potential of machine learning in vitiligo detection, several hurdles need to be overcome for further advancement. Acquisition of Diverse and Representative Datasets: Machine learning algorithms require extensive and diverse datasets to build robust models. However, obtaining comprehensive, labeled datasets covering various skin types, ages, and stages of vitiligo can pose challenges. Interpretability and Transparency: Machine learning models often function as "black boxes," making it challenging to understand the reasoning behind their predictions. Developing methods to interpret and clarify the decision-making processes of these models is essential for establishing trust and acceptance among dermatologists and patients. Integration with Clinical Workflow: Seamless integration of machine learning algorithms into clinical workflows is crucial for practical implementation. This involves creating user-friendly interfaces and ensuring compatibility with existing medical systems. These areas require focused attention to facilitate smooth adoption in clinical settings.

We present YOLO and image segmentation as unified models for precise detail recognition. Our concept aims to be straightforward and will be demonstrated through images. Unlike category-based algorithms, YOLO is trained on a holistic approach focused on recognition accuracy, where the entire image is trained together.

References

[1] Zhang, L., Mishra, S., Zhang, T., Zhang, Y., Zhang, D., Lv, Y., Lv, M., Guan, N., Hu, X. S., Chen, D. Z., & Han, X. (2021). Design and Assessment of Convolutional Neural Network Based Methods for Vitiligo Diagnosis. Frontiers in medicine, 8, 754202. https://doi.org/10.3389/fmed.2021.754202

[2] Mudunuru, V. R., & Skrzypek, L. A. (2020). A comparison of artificial neural network and decision trees with logistic regression as classification models for breast cancer survival. International Journal of Mathematical, Engineering and Management Sciences, 5(6), 1170–1190. doi:10.33889/ijmems.2020.5.6.089.

[3] S. R. Kothiyal, R. K. Ratnesh, and A. Kumar, Field Effect Transistor (FET)-Sensor for Biological Applications, International Conference on Device Intelligence, Computing and Communication Technologies, (DICCT)-2023, IEEE, 2023, 433-438.
https://doi.org/10.1109/DICCT56244.2023.10110155

[4]R. Kumar, R. K. Ratnesh, J. Singh, R. Chandra, G. Singh and V. Vishnoi, Recent Prospects of Medical Imaging and Sensing Technologies Based on Electrical Impedance Data Acquisition

ISSN:1624-1940
DOI 10.6084/m9.figshare.26090938
http://magellanes.com/

System, Journal of the Electro Chemical Society,2023, 170, 117507.https://doi.org/ 10.1149/1945-7111/ad050f

[5] Sharma, S., Guleria, K., Tiwari, S., & Kumar, S. (2022). A deep learning based convolutional neural network model with VGG16 feature extractor for the detection of Alzheimer Disease using MRI scans. Measurement. Sensors, 24(100506), 100506. doi:10.1016/j.measen.2022.100506

[6] R. Kumar, R. K. Ratnesh, J. Singh, A. Kumar and R. Chandra, IoT-Driven Experimental Framework for Advancing Electrical Impedance Tomography, Journal of Solid-State Science and Technology, 2024, 13, 027002.
https://doi.org/10.1149/2162-8777/ad2331

[7] Leachman, S. A., Hornyak, T. J., Barsh, G., Bastian, B. C., Brash, D. E., Cleaver, J. E., Cooper, C. D., D'Orazio, J. A., Fujita, M., Holmen, S. L., Indra, A. K., Kraemer, K. H., Le Poole, I. C., Lo, R. S., Lund, A. W., Manga, P., Pavan, W. J., Setaluri, V., Stemwedel, C. E., & Kulesz-Martin, M. F. (2020). Melanoma to Vitiligo: The Melanocyte in Biology & Medicine–Joint Montagna Symposium on the Biology of Skin/PanAmerican. Society for Pigment Cell Research Annual Meeting. Journal of Investigative Dermatology, 140(2), 269-274. https://doi.org/10.1016/j.jid.2019.03.1164

[8] Rushdi, R. A., & Rushdi, A. M. (2018). Karnaugh-map utility in medical studies: The case of Fetal Malnutrition. International Journal of Mathematical, Engineering and Management Sciences, 3(3), 220–244. doi:10.33889/ijmems.2018.3.3-016

[9]A. Garg, R. K. Ratnesh, R. K. Chauhan, N. Mittal, and H. Shankar, Current Advancement and Progress in BioFET: A Review, International Conference on Signal and Information Processing (IConSIP), IEEE, 2022, 1-7.
https://doi.org/10.1109/ICoNSIP49665.2022.10007517

[10] Guo, L., Yang, Y., Ding, H., Zheng, H., Yang, H., Xie, J., … Ge, Y. (2022). A deep learning-based hybrid artificial intelligencemodel for the detection and severity assessment of vitiligo lesions. Annals of Translational Medicine, 10(10), 590. doi:10.21037/atm-22-1738

[11] Ma, Z., Cai, M., Yang, K., Liu, J., Guo, T., Liu, X., & Zhang, J. (2023). Predicting the risk of autoimmune thyroid disease in patients with vitiligo: Development and assessment of a new predictive nomogram. Frontiers in Endocrinology, 14, 1109925. doi:10.3389/fendo.2023.1109925

[12]A. Garg, R. K. Ratnesh, Solar Cell Trends, and the Future: A Review, Journal of Pharmaceutical Negative Results, 2022, 13, 2051-2060.https://doi.org/10.47750/pnr.2022.13.S06.268

[13] Evgeniou, T., & Pontil, M. (2001). Support Vector Machines: Theory and Applications. In Lecture

ISSN:1624-1940
DOI 10.6084/m9.figshare.26090938
http://magellanes.com/

Notes in Computer Science. Machine Learning and Its Applications (pp. 249–257). doi:10.1007/3-540-44673-7_12

[14]M. K. Yadav, R. Kumar, R. K. Ratnesh, J. Singh, V. Vishnoi, G. Singh, A. Kumar and A. Kumar, Revolutionizing Technology with Spintronics:Devicesandtheir TransformativeApplications, Materials Science & Engineering B,
2024, 303,117293https://doi.org/10.1016/j.mseb.2024.117293

[15] Yamashita, R., Nishio, M., Do, R. K. G., & Togashi, K. (2018). Convolutional neural networks: an overview and application in radiology. Insights into Imaging, 9(4), 611–629. doi:10.1007/s13244-018-0639-9

[16] Breiman, L. (2001). Machine Learning, 45(1), 5–32. doi:10.1023/a:1010933404324

[17] Uddin, S., Haque, I., Lu, H., Moni, M. A., & Gide, E. (2022). Comparative performance analysis of K-nearest neighbour (KNN) algorithm and its different variants for disease prediction. Scientific Reports, 12(1), 6256. doi:10.1038/s41598-022-10358-x

[18] Tan, M., Pang, R., & Le, Q. V. (2019). EfficientDet: Scalable and Efficient Object Detection. doi:10.48550/ARXIV.1911.09070